POST-CLASSIFICATION OF MISCLASSIFIED PIXELS BY EVIDENTIAL REASONING: A GIS APPROACH FOR IMPROVING CLASSIFICATION ACCURACY OF REMOTE SENSING DATA

Yeqiao Wang and Daniel L. Civco
Laboratory for Earth Resources Information Systems
Department of Natural Resources Management and Engineering
U-87, The University of Connecticut
Storrs, CT 06269-4087, U.S.A.

ABSTRACT

This paper discusses an approach for extracting supporting evidence from multisource spatial data and by rule-based models to incorporate the evidence with pre-classified Landsat TM data for improving classification accuracy. The process was focused on the extracted "possibly misclassified pixels" (PMPs) only. Based on Dempster-Shafer's theory of evidence, the concepts of homogeneous, heterogeneous, and conflicting evidence and the rules for evidential combination are discussed. Boolean logic, conditional statement, and spatial relationship operations were employed in the models. By running the models, correct labels for the PMPs were judged by pooled evidence from multitemporal Landsat TM data and multisource spatial data.

KEY WORDS: Post-classification, multisource data, evidential reasoning, modeling.

1. INTRODUCTION

It is generally recognized that the improvement of classification accuracy of remote sensing data can be achieved through the incorporation of multisource digital spatial information. Through quantitative evidential reasoning, evidential combination and evidential pooling, the incorporation of ancillary spatial data as an additional source of information to be used in remote sensing data analysis and classification can be performed objectively. This paper discusses a GIS approach for improving classification accuracy. The process, based on Dempster-Shafer theory, includes two stages -- pre-classification and evidential reasoning-based post-classification.

Pre-classification involves conventional supervised classification, which typically is a statistically-based, per-pixel, spectral-data-only digital image classification approach. The purpose of the pre-classification is both to produce an initial land cover map and to obtain a basic assessment of classification accuracy. By this process, a comparatively high classification accuracy can be achieved for those areas which have significantly different spectral distributions in the remote sensing image data. However, it has been observed that some pixels will inherently and unavoidably be misclassified because of spectral mixing, particularly at the boundaries of and transitions between different classes of ground covers. These misclassified pixels are often one of the main influences on final classification accuracy.

Post-classification focuses on the evidential reasoning-based membership judgement of the "possibly misclassified pixels" (PMPs) from the initial classification. In the post-classification stage, based on the analysis of training feature overlap in n-dimensional spectral space, a question of "how many possible category labels does one PMP have?" is answered first. Then, by the support of evidence from multisource data, one possible category label is favored for each of the PMPs. Three different kinds of evidence are considered -- homogeneous evidence (evidence pointing unambiguously to a single target); heterogeneous evidence (evidence pointing to several different targets) and conflicting evidence (whereby the effect of one source of evidence is diminished by others). Homogeneous evidence can be used directly to support the existence of the related labels. It is applicable not only to the PMPs, but also to all of the other pixels favored by the evidence. Evidential combination rules are used for pooling heterogeneous and conflicting evidence from different data sources to support the existence of the favored labels.

2. DATA SOURCES AND STUDY AREAS

The multisource data in this study included two dates (May 1988 and August 1990) of geocoded Landsat Thematic Mapper (TM) images, digital elevation model (DEM) data and the derivatives of slope and aspect, digital line graph (DLG) data and their raster equivalents for transportation and hydrography. Transportation contains road information at different levels (*e.g.*, heavy duty, medium duty roads, interchanges, etc.). Hydrography data contain information on wetland areas, watersheds, shorelines, tidal mud, ditch areas, and water bodies, etc. Most of the supporting evidence in this study was supplied by those ancillary data. All multisource data layers, at the same spatial resolution, were nearly perfectly registered. The raster GIS models were developed for the evidential reasoning and the post-classification.

Six USGS $7^{1/2}$ minute quadrangles located in Connecticut were selected for developing and testing the techniques. Ellington (Q24), Middletown (Q67), and Clinton (Q98) quadrangles were used for technique development, and the adjacent quadrangles of Broad Brook (Q23), Middle Haddam (Q68), and Essex (Q99) were used for technique testing, evaluation, and refinement. The six areas range from coastal, urban-concentrated areas to hilly, agricultural and forested areas, and they represent a wide diversity of land use and land cover found in the state. This is necessary to test the extensibility and generalization of the classification methods developed. The flow chart for this study is shown in Figure 1.

3. PRE-CLASSIFICATION AND EXTRACTION OF PMPS

For deriving initial land cover data and identifying candidate pixels for the post-classification, two dates of Landsat TM images of the six quadrangles areas were classified. The May images were selected as the principal ones for classification because of better contrast and greater information content, and the August images were used as one of the ancillary data layers. Maximum likelihood classification was adopted. For the training features, 18 categories corresponding approximately to Level II of the Anderson (Anderson et al., 1976) system was selected. Some of these categories might not appear on each of the quadrangles. For example, the category of 'Tidal Mud' might appear on the coastal quadrangle areas of Essex and Clinton, but not appear on the inland quadrangle area of Ellington. The final 18 categories (C_i) are listed on Table 1. Preliminary accuracy analysis indicated that the overall accuracy of the pre-classification is approximately 83.94%.

An interactive thresholding process was adopted to determine which pixels in the classified land cover map were most likely to have been misclassified. A typical probability histogram for a classified category is shown in Figure 2. If classified pixels fell in the tail area, those pixels were spectrally far from the mean of the signature to which they were classified. Therefore, those pixels could be recognized as possibly misclassified pixels (PMPs).

Table 1. The pre-classified 18 categories

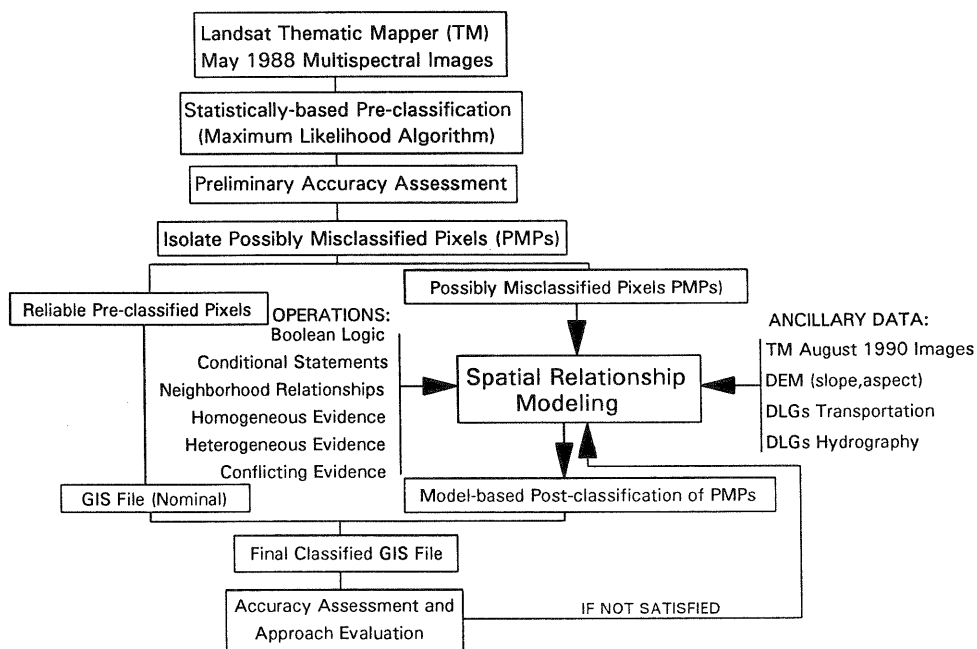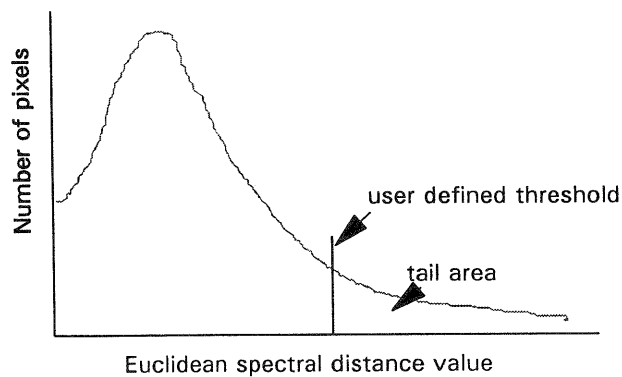|		
C_1 = High Density Residential (HDR)	C_7 = Crop Land (CL)	C_{13} = Water (WA)
C_2 = Medium Den. Residential (MDR)	C_8 = Bare Soil (BS)	C_{14} = Forested Wetland (FWL)
C_3 = Impervious surface (IMS)	C_9 = Pasture (PST)	C_{15} = Nonforested Wetland(NFWL)
C_4 = Roof (RF)	C_{10} = Deciduous Forest (DF)	C_{16} = Tidal Mud (TDM)
C_5 = Road (RD)	C_{11} = Coniferous Forest (CF)	C_{17} = Ditch Areas (DIT)
C_6 = Lawn/Gulf course/Turf (LGT)	C_{12} = Mixed Forest (MF)	C_{18} = Gravel Pits/Rocks (GPT)

Figure 1. Flow chart of the study.

Figure 2. "Cut the tail" operation on the spectral distance histogram.

Previous knowledge about training features and ground truth can be referenced to determine the threshold for each category. By applying an interactive "cut the tail" operation, 6421 pixels on Q24, 7076 pixels on Q67, and 6841 pixels on Q98 were extracted as PMPs. Those PMPs were the target of the post-classification.

4. DEMPSTER-SHAFER THEORY: NUMERICALLY-BASED EVIDENTIAL REASONING

Multisource ancillary data can supply direct or indirect evidence for identifying the correct category labels for PMPs. However, one problem for extracting evidential information is to find a way to combine the evidence from different data sources. The Dempster-Shafer theory of evidence supplies a quantitative basis for evidential combination.

In Dempster-Shafer theory, Θ denotes a finite set and is called a frame of discernment. In our case, the set of 18 possible land cover labels for PMPs comprise the frame of discernment. That is,

$$\Theta = \{HDR, MDR, IMS, RF, RD, LGT, CL, BS, PST, DF, CF, MF, WA, FWL, NFWL, TDM, DIT, GPT\}.$$

The corresponding hypothesis for Θ is that each PMP belongs to one of the 18 categories. 2^{Θ} denotes the set of all subsets of Θ. Function Bel $2^{\Theta} \rightarrow \{0, 1\}$ is called a *belief function*. Function $m : 2^{\Theta} \rightarrow \{0, 1\}$ is called a *basic probability assignment (b.p.a.)* whenever:

$$(1) \quad m(\emptyset) = 0 \quad \text{and}$$

$$(2) \quad \sum_{A \subseteq \Theta} m(A) = 1$$

The quantity $m(A)$ is the measure of the belief that is committed to A. Condition (1) indicates that there is no belief committed to the null set $\emptyset$, and (2) reveals that one's total belief has a measure of unity (Shafer, 1976). For obtaining the measure of the total belief committed to A :

$$Bel(A) = \sum_{B \subseteq A} m(B)$$

$m(B)$ is the *b.p.a.* quantity of subset B of A.

Mathematically, Dempster's rule is for computing from two or more belief functions over the same set of Θ. A new belief function called the **orthogonal sum** corresponds to the pooling of evidence. If Bel_1 and Bel_2 are two belief functions for a subset over the frame Θ with *b.p.a.* m_1 and m_2, then the probability mass for all non-empty $A \subseteq \Theta$ is defined as:

$$m(A) = \sum_{A_i \cap B_j = A} m_1(A_i)m_2(B_j)/(1 - k)$$

where:

$$k = \sum_{A_i \cap B_j = \emptyset} m_1(A_i)m_2(B_j) < 1$$

is the weight of conflict between Bel_1 and Bel_2. If Bel_1 and Bel_2 do not conflict at all, then $k = 0$. $m(A)$ gives the orthogonal sum of Bel_1 and Bel_2 and it is denoted by:

$$Bel = Bel_1 \oplus Bel_2$$

By repeating this, all of the $Bel_1, ... , Bel_n$ can be combined, i.e.

$$(((Bel_1 \oplus Bel_2) \oplus Bel_3) \oplus ... \oplus Bel_n)$$

The final **Bel** represents the pooled evidence from all Bel_i.

5. SUBSET DIVISION FOR THE FRAME OF DISCERNMENT Θ

Direct application of Dempster's rule to the frame of discernment Θ with 18 possible labels poses a computing difficulty. However, an understanding of subsets of interests can be used to reduce the complexity of numerical computation. Since unavoidable training feature overlap is one reason that causes misclassification, it is assumed that if training signatures for certain categories overlapped, then the corresponding categories should be considered to comprise one of the subsets of the Θ. The elements of the subsets represent all possible choices of category labels for certain PMPs. For example, the training features of FWL, HDR, and CL were found to overlap. This indicates that if a PMP were originally classified as FWL, it would most probably have a label as one of the above three categories. Based on this knowledge, the original hypothesis of 18 possible labels for the PMP could be narrowed to a new subset of Θ which has only three possible labels {FWL,HRD,CL}. Each element, or **singleton**, of the subsets can also be extracted as a sub-subset of the Θ. Complicated computations for probability mass among Θ, therefore, could be divided into operations on each subset, individually. Subset division is based on signature divergence analysis. Jeffries-Matusita Distance (JMD) (Swain and Davis, 1978) was adopted for analyzing the divergence between each pair of training features for selected bands. The critical upper bound JMD value of the divergence of this study was 1414. The upper bound value indicates that the corresponding signatures are totally separable in the bands being studied. JMD = 0 means that the corresponding signatures are inseparable. If $0 <$ JMD < 1414, then the training features overlap in spectral space. Table 2 shows the pairwise categories (C_i and C_j) for which the JMD $(C_i, C_j) < 1414$. If JMD $(C_i, C_j) < 1414$ for the same intersection items of C_i and C_j appeared on different band combinations, then the C_i and C_j were considered as mixed training features and the corresponding labels of C_i and C_j should be considered as elements of the subset. Twelve subsets were recognized for the Ellington quadrangle (Q24) and denoted as S_K (C_i). (where: K = 1, 2, ..., 12 represents the 12 subsets, C_i indicates that the subset is for identifying the PMPs which have originally been classified as category of C_i). The identified PMPs may have possible labels listed in the subset. For example, S_4 (C_4) = {RF,IMP,BS,GPT} signifies that subset 4 identifies the PMPs which have an originally-classified label C_4 = ROOF. Those identified PMPs may have a possible label of RF, or IMP, or BS, or GPT. The same procedure was applied to Q67 and Q98. The subsets for Θ_{Q24}, Θ_{Q67}, and Θ_{Q98} are listed on Table 3.

6. EVIDENCE POOLING AND THE POST-CLASSIFICATION

6.1 Homogeneous Evidence and the Post-classification

Homogeneous evidence is that which precisely and unambiguously supports a given singleton of subsets of Θ. In this study, some of the categories, such as RD, FWL, NFWL, TDM, DIT, etc., directly related to the corresponding information on digital line graphs (DLGs) for transportation and hydrography. For example, tidal mud is an important land cover type in coastal areas. However, because of fluctuating tidal levels, it is difficult to identify tidal flats by Landsat TM data alone. The information supplied by DLG's for hydrography can be referenced as homogeneous evidence to favor the identification of tidal flats areas. In this case, the homogeneous evidence is considered as precise, and no other controversial evidence can diminish its impacts on the support of a singleton of a subset.

Table 2. Jeffries-Matusita Distance between the categories C_i and C_j on TM band 3 vs. 4 (a), 3 vs. 5 (b), and 4 vs. 5 (c).

	C_1	C_2	C_3	C_4	C_5	C_6	C_7	C_8	C_9	C_{10}	C_{11}	C_{12}	C_{13}	C_{14}	C_{15}	C_{16}	C_{17}	C_{18}
C_1									1368	1329		1408						
C_2	1360								881	1399	1066							
C_3								1398										
C_4			1274					1339										1409
C_5																		
C_6							1318											
C_7	1413		1413	1413		1388		985			1369	1384						1407
C_8																		1289
C_9																		
C_{10}																		
C_{11}										1393								
C_{12}											1409							
C_{13}																		
C_{14}												1392						
C_{15}																		
C_{16}																		
C_{17}																		
C_{18}								1274										

(a)

	C_1	C_2	C_3	C_4	C_5	C_6	C_7	C_8	C_9	C_{10}	C_{11}	C_{12}	C_{13}	C_{14}	C_{15}	C_{16}	C_{17}	C_{18}
C_1																		
C_2	1410																	
C_3																		
C_4			1402					1405			1317							1287
C_5																		
C_6							1413			1172		1370						
C_7	1388									951	899	1406		1266				
C_8																		
C_9										1096								
C_{10}						1312												
C_{11}						1397				1308	1342							
C_{12}																		
C_{13}																		
C_{14}	1393						1208											
C_{15}																		
C_{16}																		
C_{17}																		
C_{18}								1409										

(b)

	C_1	C_2	C_3	C_4	C_5	C_6	C_7	C_8	C_9	C_{10}	C_{11}	C_{12}	C_{13}	C_{14}	C_{15}	C_{16}	C_{17}	C_{18}
C_1			1413								1333							
C_2	1403																	1413
C_3											1410							
C_4			1394					1402		1410		605		1413				1409
C_5																		
C_6							1413											
C_7								1359		1366								
C_8									1389	706	1201	1413						
C_9								1211										
C_{10}																		
C_{11}								1412	1336									
C_{12}																		
C_{13}																		
C_{14}	1413		838						1279		1394							
C_{15}																		
C_{16}																		
C_{17}																		
C_{18}								1404						1406				

(c)

Table 3. Subset division of Θ for quadrangles of Ellington (Q24), Middletown (Q67), and Clinton (Q98)

Elington quadrangle (Q24)	Middletown quadrangle (Q67)	Clinton quadrangle (Q98)
$S_1(C_1) = \{HDR,MDR,CL,FWL\}$	$S_1(C_1) = \{HDR,MDR,FWL,NFWL\}$	$S_1(C_1) = \{HDR,MDR,CL,FWL\}$
$S_2(C_2) = \{MDR,HDR\}$	$S_2(C_2) = \{MDR,PST,FWL,NFWL,MF\}$	$S_2(C_2) = \{MDR,HDR,MF\}$
$S_3(C_3) = \{IMP,RF\}$	$S_3(C_3) = \{IMS,NFWL,FWL\}$	$S_3(C_6) = \{LGT,CL\}$
$S_4(C_4) = \{RF,IMP,BS,GPT\}$	$S_4(C_6) = \{LGT,CL\}$	$S_4(C_7) = \{CL,LGT,MDR\}$
$S_5(C_6) = \{LGT,CL\}$	$S_5(C_7) = \{CL,LGT\}$	$S_5(C_{12}) = \{MF,MDR\}$
$S_6(C_7) = \{CL,LGT,BS,DF,CF\}$	$S_6(C_8) = \{BS,DF\}$	$S_6(C_{14}) = \{FWL,MDR,HDR\}$
$S_7(C_8) = \{BS,GPT,PST\}$	$S_7(C_9) = \{PST,MDR,MF\}$	$S_7(C_{15}) = \{FWL,WA\}$
$S_8(C_9) = \{PST,CF,BS\}$	$S_8(C_{10}) = \{CF,PST\}$	
$S_9(C_{10}) = \{DF,CL\}$	$S_9(C_{12}) = \{MF,MDR,PST\}$	
$S_{10}(C_{11}) = \{CF,PST\}$	$S_{10}(C_{14}) = \{FWL,MDR,HDR\}$	
$S_{11}(C_{14}) = \{FWL,HDR,CL\}$	$S_{11}(C_{15}) = \{NFWL,MDR,HDR,IMS\}$	
$S_{12}(C_{18}) = \{GPT,RF,BS\}$		

$\Theta_{Q24} = \{ S_1(C_1), S_2(C_2), S_3(C_3), S_4(C_4), S_5(C_6), S_6(C_7), S_7(C_8), S_8(C_9), S_9(C_{10}), S_{10}(C_{11}), S_{11}(C_{14}), S_{12}(C_{18}) \}$

$\Theta_{Q67} = \{ S_1(C_1), S_2(C_2), S_3(C_3), S_4(C_4), S_5(C_6), S_6(C_7), S_7(C_8), S_8(C_9), S_9(C_{12}), S_{10}(C_{14}), S_{11}(C_{15}) \}$

$\Theta_{Q98} = \{ S_1(C_1), S_2(C_2), S_3(C_3), S_4(C_7), S_5(C_3), S_6(C_{12}), S_7(C_{15}) \}$

The logical rule for using homogeneous evidence is that:

If < homogeneous evidence found > , *then* < X = C_i >

where: C_i is the homogeneous evidence supported category, X is the original label of the pre-classified pixels. The heavy duty, medium duty roads, interchanges from the transportation DLG, and tidal mud, ditch areas from the hydrography DLG were selected as homogeneous evidence. Using the ERDAS GIS modeling (GISMO) language, models with Boolean logic, conditional statements and spatial relationship operations for the pre-classified Landsat TM May 1988 data layer and other ancillary data layers were created for the evidential reasoning. Applying the models to pre-classified Landsat TM May image data, the pixels supported by homogeneous evidence from ancillary data were identified. The homogeneous evidence-supported category labels were assigned to the corresponding identified pixels. As a result, 11413 pixels (7% of the total pixels) on Q24, 22123 pixels (13.7% of the total pixels) on Q67, and 19670 pixels (12% of the total pixels) on Q98 were resolved by the homogeneous evidence and were relabled.

6.2 Heterogeneous, Conflicting Evidence and the Post-classification

Heterogeneous evidence is that which points to different singletons of subsets of Θ, (*i.e.*, two supporting pieces of evidence, one for C_i , one for C_j, with $C_i \cap C_j \neq \emptyset$.). The combining evidence provides support not only for C_i and C_j separately, but also for the conjunction $C_i \cap C_j \neq \emptyset$. Since there is no conjunction category of $C_i \cap C_j \neq \emptyset$ in our defined subsets of Θ, we have to make a choice between C_i and C_j. The heterogeneous evidence, therefore, changes to conflicting evidence with $C_i \cap C_j = \emptyset$. Conflicting evidence produces the effect that the evidence supporting C_i and the evidence supporting C_j diminish each other.

For combining evidence, basic probability assignments (*b.p.a.*) for each supporting piece of evidence on each data layer should be defined. The defined *b.p.a.*, which are numerical weights of evidence, were given numbers that represent the subjectively-judged degree of support for different categories. All supporting evidence was given the corresponding *b.p.a.*. The evidence may confirm or refute the support for certain categories. Dempster's rule of combination was then applied in combination models. By running these models, the orthogonal sums, which represent the new beliefs, were achieved. The decision rule, therefore, is that the C_i which obtained the largest orthogonal sum from supporting *b.p.a.* for each source of evidence would be favored as the label for the corresponding PMPs. The procedure reflected the accumulation of pooling total available evidence.

A set of evidential reasoning rules and a number of *b.p.a.* for each supporting piece of evidence have been defined. The reasoning rules were subset division-based. Subset $S_1(C_1)$ = {HDR MDR CL FW} of Θ_{24} is taken as an example to show the evidential reasoning results. The $S_1(C_1)$ is for identifying correct labels for the PMPs which have the pre-classified label of C_1 = HDR. Four singletons in the subset denoted that the PMPs might have four possible labels of HDR, MDR, CL and FW. Considering the results of pre-classification, it was intuitive to presume that the PMPs had 50% probability to be labeled as HDR, and 50% probability to be labeled as other categories. Since there was no clear evidence to distinguish between HDR and MDR, it was assumed that the PMPs labeled as MDR could be merged into the HDR category. Then, the PMPs have three possible labels (*i.e.*, HDR, CL, and FW). The evidential reasoning rules and the assigned *b.p.a.* were incorporated into Dempster's rule. Both conflicting weights of *k* and orthogonal sums of *b.p.a.* were computed. An example for computing conflicting weights and orthogonal sums, which deals with the resolution "HDR = Yes" on the evidential layer of classified Landsat TM August 1990 image, is shown in Figure 3.

The given *b.p.a.*, orthogonal sum computation and the supporting evidence pooling among evidential layers all were achieved by applying the reasoning model. In the model, PMPs and each evidential layer were defined as input files. The pre-assigned *b.p.a.* were defined as floating point parameters. Depending on the requirements, intermediate variables were defined either in floating point or integer format. Aside from arithmetic calculations, typical Boolean logic and conditional statement operations in the model are:

output = *either* X1 if input 1 *and* input 2 *and* ... is true, *or* X2 *otherwise*;

and

output = *conditional* { (condition 1 is true) X1
(condition 2 is true) X2
- - -
(default) user defined};

The entire process of defining *b.p.a.* and computing orthogonal sums for the subset $S_1(C_1)$ is shown in Figure 4. A set of similar models was developed for each of the subsets of the Θ. Totally, 17834 pre-classified pixels, approximately 11% of the total pixels in Q24, 29199 pre-classified pixels, approximately 18% of the total pixels in Q67, and 26511 pre-classified pixels, approximately 16% of the total pixels in Q98 were post-classified by either homogeneous evidence or conflicting evidence-supported information.

7. ACCURACY ASSESSMENT

For accuracy assessment, the three quadrangles of Ellington, Middletown, and Clinton were selected. Those quandrangles are the representatives for the agricultural, hilly, forested areas, urban concentrated areas, and coastal areas, respectively. Three hundred reference pixels were randomly selected for each of the quadrangles.

	m(a1) = 0.5	m(a2) = 0.5
mr(b1) = 0.6	$mr1 = \dfrac{m(a1) * mr(b1)}{1 - k1}$ = 0.375	k2 = m(a2)*mr(b1) = 0.3
mo(b1) = 0.4	k1 = m(a1)*mo(b1) = 0.2	$mo1 = \dfrac{m(a2) * mo(b1)}{1 - k2}$ = 0.286

Figure 3.   Example of computing conflicting weights and orthogonal sums

PMPs with pre-classified labels of HDR/
MDR on Landsat TM May 1988 image

b.p.a. define
$m(a1) = 0.5$
$m(a2) = 0.5$

HDR = Yes   HDR = No

Evidential supporting layer 1:
Classified Landsat TM
August 1990 image

b.p.a. define
$mr(b1) = 0.6$
$mo(b1) = 0.4$

Orthogonal Sum
$mr1 = .5*.6/.8 = .375$
$mo1 = .5*.4/.7 = .286$

b.p.a. define
$mr(b2) = 0.4$
$mo(b2) = 0.6$

Orthogonal Sum
$mr2 = .5*.4/.7 = .286$
$mo1 = .5*.6/.8 = .375$

Evidential supporting layer 2:
DLG's Hydrography data

FW = Yes   FW = No   FW = Yes   FW = No

b.p.a. define
$mr(c1) = 0.3$
$mo(c1) = 0.2$
$mf(c1) = 0.5$

b.p.a. define
$mr(c2) = 0.5$
$mo(c2) = 0.2$
$mc(c1) = 0.3$

b.p.a. define
$mr(c3) = 0.2$
$mf(c2) = 0.5$
$mc(c2) = 0.3$

b.p.a. define
$mr(c4) = 0.2$
$mf(c3) = 0.3$
$mc(c3) = 0.5$

Orthogonal Sum   Orthogonal Sum

$mr3 = .1525$ $mr4 = .1523$ $mr5 = .074$ $mr6 = .044$
$mo3 = .074$ $mo4 = .074$ $mf2 = .231$ $mf3 = .1525$
$mf1 = .1667$ $mc1 = .107$ $mc3 = .1525$ $mc3 = .231$

Evidential supporting layer 3:
DEM derived Slope
Is slope > 5 degrees ? Yes   No   Yes   No

b.p.a. define
$mr(d1) = 0.5$
$mf(d1) = 0.3$
$mc(d1) = 0.2$

No Change

b.p.a. define
$mr(d2) = 0.3$
$mf(d2) = 0.2$
$mc(d2) = 0.5$

No Change

Orthogonal Sum   Orthogonal Sum

$mr7 = .0825$ $mr8 = .0234$
$mo5 = .0157$ $mf4 = .0567$
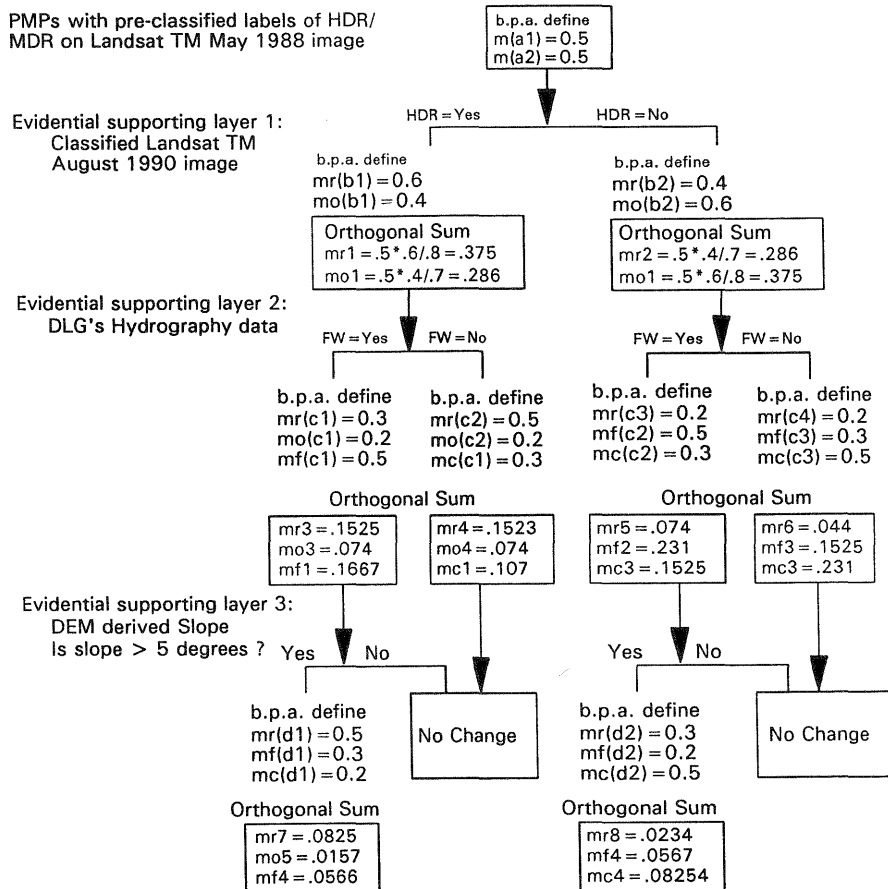$mf4 = .0566$ $mc4 = .08254$

Figure 4. Orthogonal sums by considering different evidential layers.
(mr* is the orthogonal sum for supporting HDR, mo* for supporting Others,
mf* is the orthogonal sum for supporting FW, mc* for supporting CL.)

By referencing the "ground truth" data supplied by aerial photographs, topographic and thematic maps, field observations and the investigator's familiarity of the ground cover types, the agreement of the randomly selected sample pixels and the ground truth were analyzed. Final results show that overall post-classified accuracy are 88.3% for the Elington quadrangle, 89.3% for Middletown quadrangle, and 88.6% for Clinton quadrangle, respectively. Additionally, the visual appearance of spatial features on the post-classified images is much more clear than they are in the pre-classified images. Linear features such as different levels of transportations, ditches, shorelines, coastal lines, and areal features such as wetland areas, tidal mud areas, agricultural areas, etc., are continuously linked and quite distinguishable. It is obvious that by handling the PMPs not only has the classification accuracy has been improved, but so has the legibility of the land cover maps.

8. CONCLUSIONS

This paper demonstrates how spatial relationships among multisource data layers may be formulated as a knowledge base and processed using rule-based evidential reasoning models. The advantages of the approach are as follows:

• By partitioning the process into pre-classification and post-classification, the approach focuses on the possibly misclassified pixels (PMPs) and the homogeneous evidence-related pre-classified pixels only.

Approximately 80% of the pre-classified pixels have been recognized as having acceptable preliminary classification accuracy. For those presumably correctly labeled pixels, there need be no post-classification refinement. It is efficient to improve the classification accuracy by handling PMPs only instead of processing all image pixels.

• The evidential reasoning-based post-classification approach provides a scheme that can readily pool spatial information from multisource data. It can be certain that multisource spatial data would supply reliable confidence from different features to help the judgement of correct labels for the PMPs. The approach is efficient for handling the problem areas and classes caused by insufficient information of remote sensing data and incomplete knowledge of the training features in the conventional statistically-based classification.

• The post-classification was achieved by a set of models with each focused on one subset of the Θ. Basically, the difference among those models was the pre-assigned *b.p.a.* parameters for different evidence, the input evidential data layers, and the evidential reasoning rules. The models were stored in a GIS model library. Whenever additional new data layers become available, the models can be easily updated by changing or adding *b.p.a.* parameters or inserting new Boolean logic or conditional statement operations.

85

- The evidential reasoning rules were expert knowledge based. A rule-based solution gave a new level of flexibility when facing different classification problems. The evidential reasoning rules and the models could be integrated into knowledge-based GIS in the future. The expert knowledge could be used to update or reform the reasoning rules and models, so that the up-to-date output from both multisource spatial data and available expert knowledge in the system could be achieved.

We also noticed the limitations of the approach. The membership judgement for PMPs depends on the multisource spatial data. Although it can be certain that more different spatial data in compatible digital form will be available in the future, however, the difficulties of finding optimal evidence to distinguish among some of the confused categories will remain. Therefore, the analysis based solely on the PMPs' corresponding attribute labels on multisource spatial data layers is not enough. We should consider not only the corresponding attributes of the PMPs on different spatial data layers, but also the spatial attributes of the neighborhood of the PMPs (Wang and Civco, 1992).

9. ACKNOWLEDGMENTS

10. REFERENCES

Anderson, J.R., E.E. Hardy, J T. Roach, and R.E. Witmer, 1976. A Landuse and Landcover Classification System for Use with Remote Sensing Data, U.S. Geological Survey Professional Paper 964. pp. 8-9.

Shafer, G. 1976. A Mathematical Theory of Evidence. Princeton University Press. p. 38.

Swain, Philip H. and Shirley M. Davis. 1978. Remote Sensing: The Quantitative Approach. McGraw Hill Book Company, New York.

Wang, Y. and D.L. Civco. 1992. Spatial Modeling-based Post-classification of Satellite Remote Sensing Data for Improved Land Cover Mapping. Proceedings of ASPRS/ACSM/RT'92 Convention, August 3 - 7, 1992, Washington D.C..